

SBI/IFUSP
BASE: 04
SYS Nº: 1080546



Instituto de Física Universidade de São Paulo

Magnetoconductance of two Independently Tunable Parallel Point Contacts Using an Elliptical Antidot

Kleber, X.; Cassé, M.; Portal, J.C.

*Grenoble High Magnetic Field Laboratory, MPI-FKF and CNRS,
Grenoble, França
INSA-Toulouse, Toulouse, França*

Gusev, G.M.

*Instituto de Física da Universidade de São Paulo, São Paulo,
Brasil*

Budantsev, M.V.; Maude, D.K.

*Grenoble High Magnetic Field Laboratory, MPI-FKF and CNRS,
Grenoble, França*

Gennser, U.

Paul Scherrer Institute, Villigen-PSI, Switzerland

Kvon, Z.D.; Plotnikov, A.E.; Toropov, A.I.; Moshegov, N.T.

*Institute of Semiconductor Physics, Russian Academy of Sciences,
Siberian Branch, Novosibirsk, Russia*

Publicação IF - 1369/99

UNIVERSIDADE DE SÃO PAULO

Instituto de Física

Cidade Universitária

Caixa Postal 66.318

05315-970 - São Paulo - Brasil

Magnetoconductance of Two Independently Tunable Parallel Point Contacts Using an Elliptical Antidot

X.Kleber^{1,2}, G.M.Gusev³, M.V.Budantsev¹, M.Cassé^{1,2},
U.Gennser⁴, D.K.Maude¹, J.C.Portal^{1,2}, Z.D.Kvon⁵,
A.E.Plotnikov⁵, A.I.Toropov⁵, N.T.Moshegov⁵

¹*Grenoble High Magnetic Field Laboratory, MPI-FKF and CNRS,
BP 166, F-38042 Grenoble Cedex 9, France*

²*INSA-Toulouse, F-31077 Toulouse, France*

³*Instituto de Física da Universidade de São Paulo, SP, Brazil*

⁴*Paul Scherrer Institute, CH-5232 Villigen-PSI, Switzerland*

⁵*Institute of Semiconductor Physics, Russian Academy of Sciences,
Siberian Branch, Novosibirsk, Russia*

Magnetoconductance measurements have been made on a system composed of a lithographically defined elliptically shaped antidot placed in the center of a constriction defined by two lateral gates in a normal GaAs/AlGaAs heterostructure. We observe a step in the conductance as the gate voltage is varied resulting from the depopulation of the subband in each of the two Quantum Point Contact (QPC). When one of the lateral gates is swept, quantized steps at integer multiples of $2e^2/h$ are observable, while when the two gate voltage are varied, quantized step at integer multiples of $4e^2/h$ appears, revealing the additivity of the conductance of each QPC. At low magnetic field, the trapping of stable trajectories around the antidot can be seen leading to peaks in the magnetoresistance. Using a magnetic billiards formalism, we have calculated the dynamics in the phase space of a particle colliding around an elliptic antidot. The specific shape of the antidot, i.e. elliptic, allows a mixing between the periodic and the chaotic components to develop, and thus the magnetic field induced changes in the phase space lead to observable anomalies.

1. Introduction

Advances in nanofabrication have made possible the investigation of electronic transport in the ballistic regime. One of the most remarkable manifestations of confinement is the quantized conductance observed in a Quantum Point Contact (QPC) [1]. As the voltage is varied, the number of occupied subbands in

the narrow constriction changes, leading to observable steps in the conductance at integer multiples of $2e^2/h$.

When sweeping the magnetic field through low values, where the size of the cyclotron radius is comparable with the size of the antidots, fluctuations in the resistance occur. Transport anomalies in an array of elliptical antidots have already been reported [2], which are due to the trapping of an electron around a single antidot. The specific shape of the antidot, i.e. elliptic, allows a mixing between quasi-periodic, periodic and chaotic trajectories to develop in the phase space.

In this paper, we investigate such anomalies for two different orientations of a single elliptic antidot, (i) the long axis parallel to the current direction (longitudinal) and (ii) the long axis perpendicular to the current direction (transverse). We compare these anomalies for the two configurations and explain them by calculating the fraction of stable orbits.

2. Experiments

Samples were prepared in a modulation doped AlGaAs/GaAs heterostructures with a carrier concentration $2-4 \times 10^{15} \text{ cm}^{-2}$ and a mean free path $l_e \approx 10 \mu\text{m}$. A single elliptically shaped antidot was created in the center of the constriction using electron beam lithography and reactive plasma etching. Figure 1 shows a Scanning Electron Microscope pictures of the device for an antidot with the long axis perpendicular to the current direction. The samples with a long axis parallel to the current direction have also been created. The lithographic length of the antidot is $1 \mu\text{m}$ with a width of $0.3 \mu\text{m}$, whereas the width of the constriction is $2.4 \mu\text{m}$ (between the two lateral gates).

The experiments were performed in a dilution refrigerator, at a temperature of 50 mK and in a He⁴ cryostat at a temperature of 4.2K. Standard four terminal measurement techniques were used, with the bias across the device low enough to avoid electron heating. The magnetic field was applied by means of a superconducting magnet.

3. High Magnetic Field Results

At high magnetic fields, transport occurs via edge states on each side of the sample. For integer fillings factor, the transverse resistance exhibits plateaux whereas a minima occurs in the longitudinal resistance (R_{4T}). The presence of the antidot slightly modifies this picture as the density in the constriction n_c , and thus the filling factor ν_c , are not equal to the density in the wide region n_w (filling factor ν_w). By changing the voltage of the lateral gate, we are able to

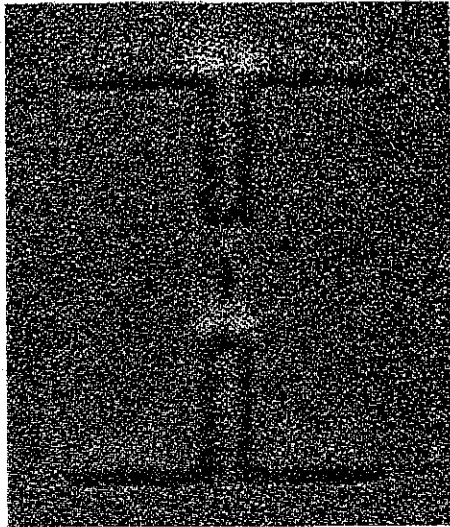


Figure 1. SEM image of the sample. The length of the antidot is $1\mu\text{m}$ and the width of the constriction is $2.4\mu\text{m}$.

modify the concentration in the constriction, in order to have an integer filling factor in the wide part of the sample and in the constriction. Using a Landauer-Büttiker formalism, one can express the four terminal resistance (R_{4T}) of the device assuming that $\nu_w - \nu_c$ spin resolved edge states are reflected by the antidot potential [3–5]:

$$R_{4T} = (h/e^2) [1/\nu_c - 1/\nu_w]. \quad (1)$$

Figure 2a shows the (R_{4T}) of the device as a function of B at a temperature of 50 mK for different values of the gate voltage. We observe two plateaux at magnetic field values of $B=4.3$ T and $B=2.15$ T corresponding to $\nu_c=2$ $\nu_w=3$, and $\nu_c=4$ $\nu_w=6$ respectively. The quantized values are in excellent agreement with the values expected from Eq. (1), i.e. 4300Ω and 2150Ω . In the inset of Fig. 2a, we have represented the edge state reflected by the constriction corresponding to these two plateaux.

This difference in filling factor corresponds to a carrier concentration in the wide and in the constriction region equal to $n_w = 3.15 \times 10^{15} \text{ cm}^{-2}$ and $n_c = 2.1 \times 10^{15} \text{ cm}^{-2}$. This assignment is also supported by the existence of a second peak in the Fourier Transform of the Shubnikov-de Haas oscillation (reciprocal space) corresponding to a fundamental magnetic field equal to $B=8.6$ T ($\nu_c=1$ and $n_c = 2.1 \times 10^{15} \text{ cm}^{-2}$) (see Figure 2b). As the filling factor is never the same in the wide region and in the region of the constriction, the SDH oscillations are a

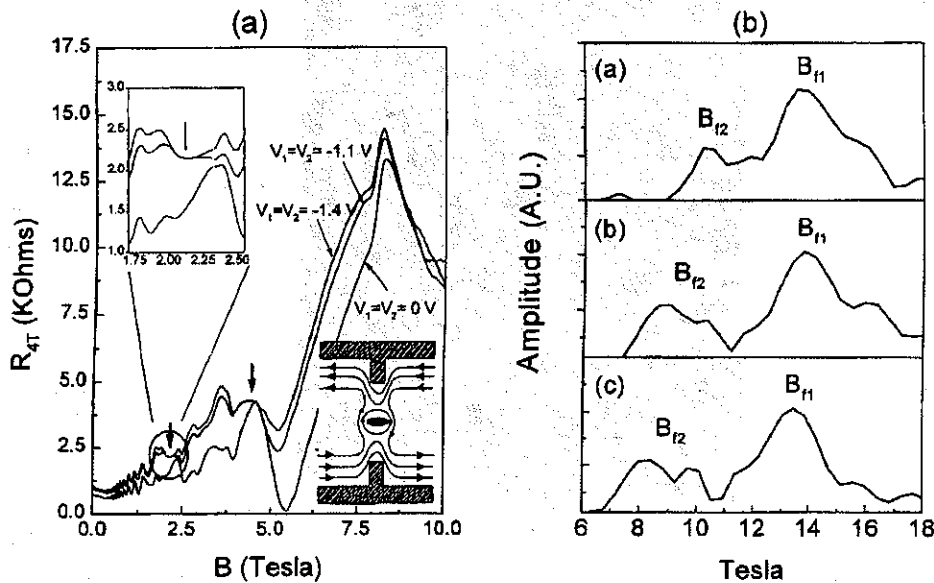


Figure 2. (a) Four terminal resistance of the sample with horizontal antidot at $T=50$ mK for different values of the gate voltage ($V_1=V_2=0$ V, $V_1=V_2=-1.1$ V, $V_1=V_2=-1.4$ V). The upper inset shows an enlarged view of the plateau at $B=2.15$ T. The lower inset shows the reflected edge channel in the constriction. (b) Fourier transform of the Shubnikov-de Haas oscillations for three values of the gate voltage (curve a $V_1=V_2=0$ V, curve b $V_1=V_2=-1.1$ V, curve c $V_1=V_2=-1.4$ V). As the negative voltage is increased, the second peak B_{f2} is shifted to the lower magnetic field.

superposition of the two components with two different fundamental period B_{f1} and B_{f2} , with a plateau appearing each time the ratio n_c/n_w can be expressed as a ratio of rational numbers.

We do not observe any Aharonov-Bohm fluctuations, nor resonant tunneling between bound states around the antidot and the edge states along the channel. A possible explanation is the non-perfect symmetry between the two constriction defined by the antidot and the gate. With previous devices of a similar design, the Aharonov-Bohm oscillations were absent or a few were observed [5,6], mainly due to the lack of ideal symmetry. Simpson et al [7], by fine tuning the constriction have reported very clear AB oscillations with a very high peak-to-valley ratio.

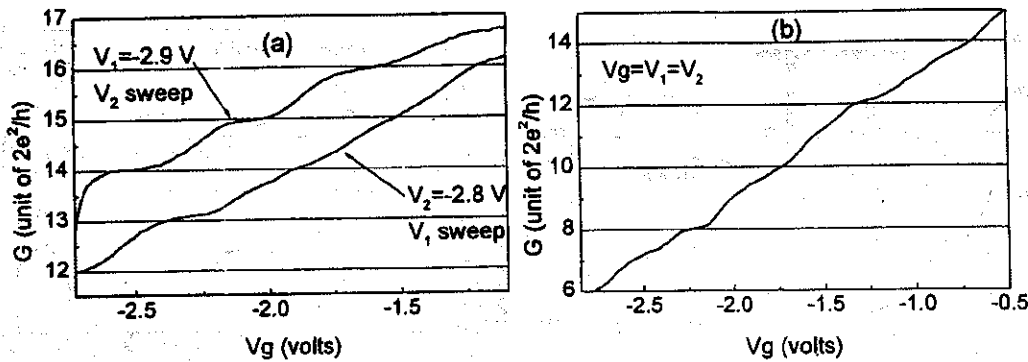


Figure 3. Conductance extracted from the resistance for (a) each of the two QPCs, and (b) for the two QPCs simultaneously.

4. Zero Magnetic Field Results: two QPC's in parallel

Recently, two QPC in parallel have experimentally demonstrated the additivity of each QPC, producing quantized step at integer multiples of $4e^2/h$ [6–8] when both QPC depopulate simultaneously. These experimental results confirmed the Castaño and Kirczenow's theoretical calculation concerning the additivity of parallel QPC conductivity [9]. Even when the two QPC are not perfectly symmetrical, Smith et al observed $4e^2/h$ steps in the conductance and argue that to minimize the energy of the coupled system, an exchange of carriers between the channels leads to a simultaneous depopulation of the two QPC, and thus to quantized step at integer value of $4e^2/h$ [6]. These result were not confirmed by Simpson et al who observed that the two QPC depopulate independently, even when a magnetic field was applied [7].

By sweeping independently the two lateral gates, we can either have one or two QPC in parallel. When one of the gates is fixed at a negative value in order to nearly pinch off one point contact, the resistance is dominated by the conductance of the second QPC. Thus, one should obtain quantized step in the conductance at $2e^2/h$.

Figure 3a shows the conductance obtained from the four terminal resistance after subtracting the background resistance when one of the two QPC is kept at a fixed voltage. We can clearly see the $2e^2/h$ step due to the depopulation of the electric subband in the constriction as the gate voltage is swept. Note that the QPC depopulate simultaneously, and by sweeping the two gates we observe the $4e^2/h$ quantized step (Figure 3b). As the two QPC depopulate simultaneously, we cannot make any conclusions on the existence of correlations in the depopulation due to the interaction between the two QPC as mentioned

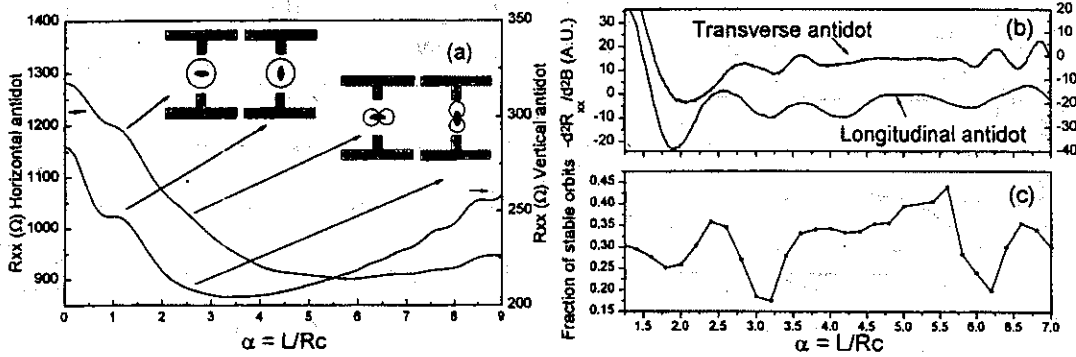


Figure 4. (a) represents the two magnetoresistance curves for the two configurations, i.e. for a transverse and a longitudinal antidot. In the inset, we show typical orbits which are mainly responsible for the increase in the resistance indicated by the corresponding arrows. (b) second derivative of the magnetoresistance for a transverse and longitudinal antidot, and (c) corresponding calculated fraction of stable orbits around a single elliptic antidot.

by Smith et al [6].

5. Low Magnetic Field Regime: Magnetic Billiards

At low magnetic field, we observe fluctuations in the magnetoresistance which we attribute to the pinning of electrons around the single antidot. When the size of the cyclotron radius is comparable with the size of the antidot, pinning mechanism can occur, leading to a peak in the magnetoresistance. To validate this hypothesis, we have calculated the dynamics of a particle colliding with an elliptically-shaped antidot using a magnetic billiards formalism [2]. Figure 4c shows the resistance at low magnetic field obtained for the two directions of the elliptic antidot, and in figure 4a we have extracted the small anomalies by computing the second derivative as a function of the dimensionless magnetic field ($\alpha=L/R_c$ where L is the length of the antidot and R_c the cyclotron radius). We can see clear reproducible oscillations which we attribute to pinned electron orbits around the antidot, as sketched for example in the inset of figure 4c.

Assuming a hard wall potential for the antidot, we have calculated in figure 4b the dynamics of the particle in the phase space by extracting the fraction of stable orbits using computation of the Lyapunov exponent (details of the method used can be found in Ref. [2]). The agreement is quite good even if some of the parameters such as the local electron density and the length of the

antidot are not known with sufficient precision.

Finally, as these magnetoresistance anomalies apparently remain independent of the direction of the antidot, it proves that independently of the current direction, pinning mechanisms around single antidots can occur in an electric field as long as it is low enough to avoid destruction of quasi-periodic orbits.

References

- [1] B.J.van Wees, H.van Houten, C.W.J.Beenakker, J.G.Williamson, L.P.Kouwenhoven, D.van der Marel, and C.T.Foxon, *Phys. Rev. Lett.*, 60 (1988) 848.
- [2] X.Kleber, G.M.Gusev, U.Gennser, D.K.Maude, J.C.Portal, D.I.Lubyshev, P.Basmaji, M.de P.A.Silva, J.C.Rossi, and Yu.V.Nastaushev, *Phys. Rev.*, B54 (1996) 13859.
- [3] S.Washburn, A.B.Fowler, H.Schmid, and D.Kern, *Phys. Rev. Lett.*, 61 (1988) 2801.
- [4] R.J.Haug, A.H.MacDonald, P.Streda, and K.von Klitzling, *Phys. Rev. Lett.*, 61 (1988) 2797.
- [5] S.W.Hwang, J.A.Simmons, D.C.Tsui, and M.Shayegan, *Phys. Rev.*, B44 (1991) 13497.
- [6] C.G.Smith, M.Pepper, R.Newbury, H.Ahmed, D.G.Hasko, D.C.Peacock, J.E.F.Frost, D.A.Rotchie, G.A.C.Jones, and G.Hill, *J. Phys.: Condens. Matter*, 1 (1989) 6763.
- [7] P.J.Simpson, D.R.Mace, C.J.B.Ford, I.Zailer, M.Pepper, D.A.Ritchie, J.E.F.Frost, M.P.Grimshaw, and G.A.C.Jones, *Appl. Phys. Lett.*, 63 (1993) 3191.
- [8] C.Gould, A.S.Sachrajda, Y.Feng, A.Delage, P.J.Kelly, K.Leung, and P.T.Coleridge, *Phys. Rev.*, B51 (1995) 11213.
- [9] E.Castaño, and G.Kirczenow, *Phys. Rev.*, B41 (1990) 5055.